The Third Body Concept /D. Dowson et al. (Editors)
1996 Elsevier Science B.V.

Role of the Third Body in Life Enhancement of MoS_2

K.J. Wahl and I.L. Singer

Code 6170, US Naval Research Laboratory, Washington, DC 20375-5342 USA

A lubrication replenishment process that accounts for the long life of MoS_2 coatings worn heavily early in sliding is described and quantified. Reciprocating sliding of a steel ball against MoS_2 coated flats was performed using a new test methodology called 'stripe testing' to monitor wear evolution. Worn surfaces were characterized with optical (Nomarski) and Michelson (interference) microscopy, as well as energy dispersive X-ray spectroscopy. Two important 'third-bodies,' the ball transfer films and compacted debris patches at track turnaround points, were identified. Material transfer between the track and ball surfaces acts as a reservoir of solid lubricant and plays an important role in sustaining lubricated sliding of MoS_2. Dynamics of the process were inferred from measurements of third-body material loss and buildup on track and ball surfaces.

1. INTRODUCTION

MoS_2 coatings, typically ≤1 μm in thickness, can provide ultra-low friction lubrication for sliding or rolling contact under moderate loads and extreme sliding conditions (e.g. vacuum, space). Interestingly, thin coatings of MoS_2 can withstand hundreds of thousands of sliding cycles, having overall wear rates <<1 nm/cycle. Although some of this behavior can be explained in terms of the bulk mechanical properties of MoS_2 (e.g. low friction coefficient in terms of the plasticity/shear strength), the high endurance has never been accounted for. Furthermore, while MoS_2 provides endurant sliding, it is well known that most of the coating is lost early in life, both in sliding [1,2,3,4] and rolling [5]. How, then, does the remaining lubricant sustain sliding? And, how can we study the wear behavior of a solid lubricant with such low wear rates?

We address these issues using MoS_2 coatings prepared by ion-beam assisted deposition (IBAD). Specifically, we have examined how a coating, worn heavily early in sliding, is able to endure the remaining 90% of sliding life. Wear and material transfer were monitored and quantified by coupling a specialized reciprocating wear test with analytical thickness measurements of third-body interfacial films. A lubrication replenishment process is proposed and the role of the third-body in transfer and replenishment is discussed.

2. EXPERIMENTAL

Thin, dense MoS_2 coatings were deposited by the IBAD technique [6,7] to thicknesses from 285 to 1020 nm on hardened steel substrates. A thin (30-40 nm) TiN interlayer was present to act as a diffusion barrier during deposition [8]. Six different MoS_2 coatings were examined in this study; the results for one of these coatings (320 nm thick) are reported in detail in this paper. Reciprocating sliding experiments were performed at 3-4 mm/s sliding speed in a dry air environment (RH<2%) with 6.4 mm diameter 52100 steel balls. The initial load was fixed at 9.8 N (mean Hertzian pressure of 0.92 GPa).

Wear tests were performed using a reciprocating sliding test methodology, diagrammed in Figure 1 and hereafter referred to as "stripe testing." In this methodology, a series of sliding tests were performed to various fractions of sliding life; a new ball was used for each successive track. Individual tracks were run a length of 5 mm for the first n = {1, 3, 10, 30, 100, ...} cycles; then, the stroke length was shortened to 3 mm for an additional $2n$ cycles. Tests performed in this manner result in tracks containing three turnaround points (one at each end and one in the middle), and adjacent tracks had segments worn to duplicate sliding cycles. Friction coefficients were monitored throughout the tests, and failure (if reached) was

Report Documentation Page

Form Approved
OMB No. 0704-0188

1. REPORT DATE	2. REPORT TYPE	3. DATES COVERED
1996		**00-00-1996 to 00-00-1996**

4. TITLE AND SUBTITLE	5a. CONTRACT NUMBER
Role of the Third Body in Life Enhancement of MoS2	5b. GRANT NUMBER
	5c. PROGRAM ELEMENT NUMBER
6. AUTHOR(S)	5d. PROJECT NUMBER
	5e. TASK NUMBER
	5f. WORK UNIT NUMBER
7. PERFORMING ORGANIZATION NAME(S) AND ADDRESS(ES) **Naval Research Laboratory,Code 6170,4555 Overlook Avenue, SW,Washington,DC,20375**	8. PERFORMING ORGANIZATION REPORT NUMBER
9. SPONSORING/MONITORING AGENCY NAME(S) AND ADDRESS(ES)	10. SPONSOR/MONITOR'S ACRONYM(S)
	11. SPONSOR/MONITOR'S REPORT NUMBER(S)

12. DISTRIBUTION/AVAILABILITY STATEMENT
Approved for public release; distribution unlimited

13. SUPPLEMENTARY NOTES

14. ABSTRACT

15. SUBJECT TERMS

16. SECURITY CLASSIFICATION OF:			17. LIMITATION OF ABSTRACT	18. NUMBER OF PAGES	19a. NAME OF RESPONSIBLE PERSON
a. REPORT **unclassified**	b. ABSTRACT **unclassified**	c. THIS PAGE **unclassified**		**7**	

1996 Elsevier Science B.V.

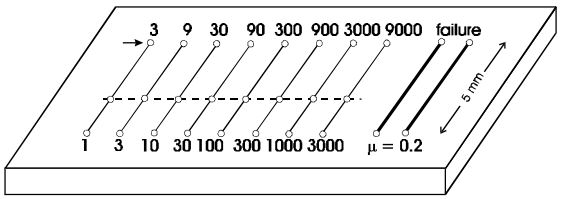

Figure 1. Schematic of reciprocating sliding 'stripe' testing series for this wear study. Arrow shows ball starting location, turnaround points are indicated by circles, and sliding cycles for the track segments are numbered.

defined as the number of sliding cycles attained before the average friction coefficient reached 0.2.

After the sliding tests, wear tracks and ball transfer films were examined by optical (Nomarski) microscopy. Track depths were measured via Michelson interference (MI) microscopy and are reported as maximum track depths. Thickness of wear tracks, debris patches at turnaround points, and ball transfer films were estimated by energy dispersive X-ray spectroscopy (EDS) using a thin window Tracor Northern system. EDS spectra were acquired at beam energies of 10 and 20 keV, beam current of 2.0 nA and detector take-off angle of 25°. At these energies, the sampling depths are ~0.75 and 2.6 μm, respectively (see e.g. Ehni and Singer [9]). Since the Mo L_α and S K_α X-ray peaks overlap around 2.3 keV, the combined X-ray signal intensity, I_{Mo+S}, was used to quantify MoS_2 coating thickness. Area analysis was used to obtain average thickness values of worn surfaces. Conversion of I_{Mo+S} to thickness was accomplished using a stepped thickness coating of MoS_2 deposited on Si [see Appendix]; I_{Mo+S} was approximately linear with coating thickness for thicknesses less than ~500 nm at 20 keV and ~120 nm at 10 keV.

3. RESULTS

3.1 Coating Wear

Reciprocating sliding stripe tests were performed on 6 coatings that had better than average sliding endurance in rotating pin-on-disk tests [10]. Friction coefficients remained low throughout testing (0.02-0.06) until late in sliding life. After testing, wear track depths were measured by MI. For all the MoS_2 coatings, sliding for fewer than 100 cycles resulted in little or no measurable wear. By 3000 cycles, all of the coatings tested had substantial coating loss.

A MoS_2 coating demonstrating typical wear behavior is shown in Figure 2 [11]. The wear behavior can be divided into three distinct stages.

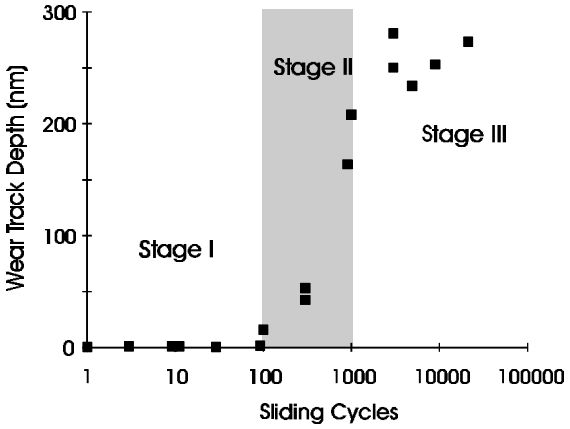

Figure 2. IBAD MoS_2 coating wear track depths measured by interference microscopy.

For the first 100 cycles, there was no measurable wear (Stage I). A period of rapid wear follows (Stage II), where the coating is worn to nearly the full thickness by ~1000 cycles. A long period of low average wear is then observed during the remaining ~20000 cycles (Stage III).

3.2 Third bodies — wear tracks

Figure 3 shows a montage of optical micrographs displaying the wear tracks between 100 cycles and failure. Before 100 cycles (not shown), the tracks had a lightly burnished appearance and a small amount of material deposited at the track ends. From 100 to 300 cycles, light scratches were visible on the track. Patches of compacted debris were visible at the track ends, and ejected debris particles were observed along the sides of the tracks and beyond the compacted debris at the track ends. Between 300 and 1000 cycles, larger patches of material were seen in the track and at the ends of the track, and scratches were more pronounced. By 3000 cycles, darker (brown) regions were observed in the track, suggesting that the coating was worn through to the TiN interlayer. Scratches remained pronounced over the entire

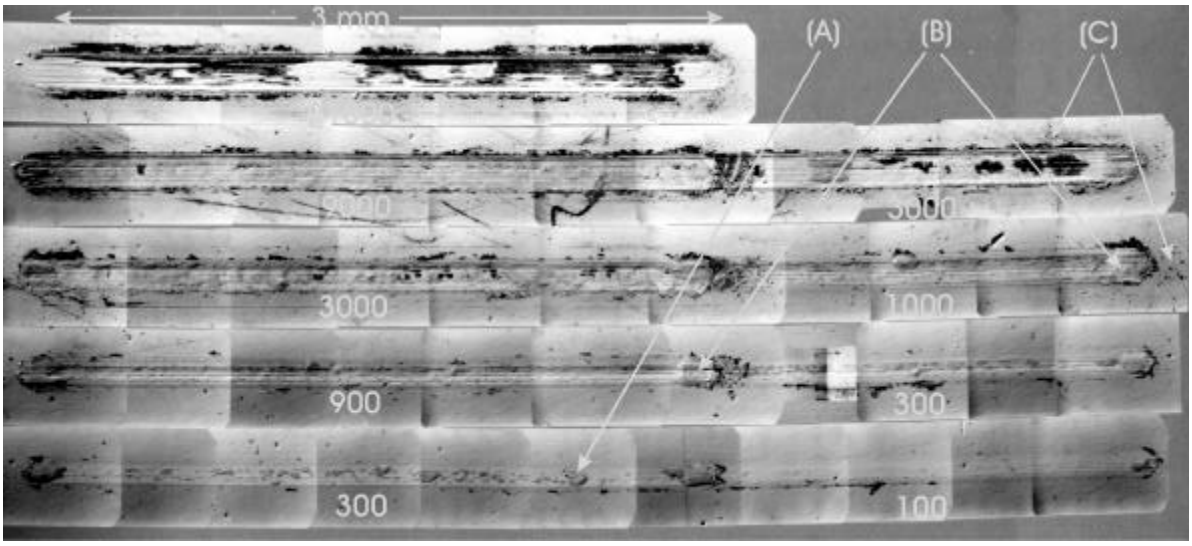

Figure 3. Montage of optical micrographs of wear tracks showing evolution of IBAD MoS_2 wear track morphology between 100 cycles and failure.

track surface. Compacted and loose debris remained visible along the sides and at the ends of the track; debris patches at track ends were less pronounced. At failure, while some regions still appeared to have intact coating, long strips of the dark areas (TiN interlayer) as well as bright white areas were visible.

In Figure 3, tracks worn to comparable sliding cycles are positioned adjacent (but offset diagonally) to each other. First, note the consistency of the morphologies exhibited in the two 300 cycle tracks, the 900 and 1000 cycle tracks, and the two 3000 cycle tracks. In this arrangement, it can be seen that the amount of compacted and loose debris deposited at the ends of the wear tracks increased with sliding cycle until 3000 cycles; after this, the compacted debris was depleted as sliding progressed. The loose debris ejected from the track is excluded from further participation in the sliding process.

Several types of third bodies were identified from the optical microscopy of track surfaces; examples of these are pointed out in Figure 3. These included lumps of compacted debris on the wear track surface (A), large patches of debris at turnaround points (B), and small (<10 μm) debris particles along the sides and at the extreme ends of the wear scars (C). It is important to note that the patches of material observed at the ends of the tracks are *directly* under the turnaround points, and *not* beyond the turnaround points; the ball rests over these points during each cycle. Together, the individual third bodies make up the distinct morphologies associated with each identified stage of wear. (A more detailed examination of wear track morphology and chemistry will be published elsewhere).

3.3 Third bodies — transfer films on balls

Transfer films on ball surfaces were distributed in three distinct regions of the contact [12], and a number of third bodies were identified. The progression of third body formation on the ball surfaces was correlated to the 3 stages of wear; like the track surfaces, each stage had a distinct morphology. During the first few sliding cycles (Stage I, not shown), very thin films of MoS_2 transferred to the center of the contact (determined by AES [11]). Thicker patches of compacted debris were observed around the perimeter of the contact zone. During Stage II, the center of the contact zone acquired small lumps of debris (Figure 4a) and by Stage III, the film had become a continuous, thick transfer pad (Figure 4b). Copious amounts of loose debris were observed around the contact zone on the ball surface by Stage II, accumulating as sliding progressed.

3.4 Quantification of wear and third body evolution

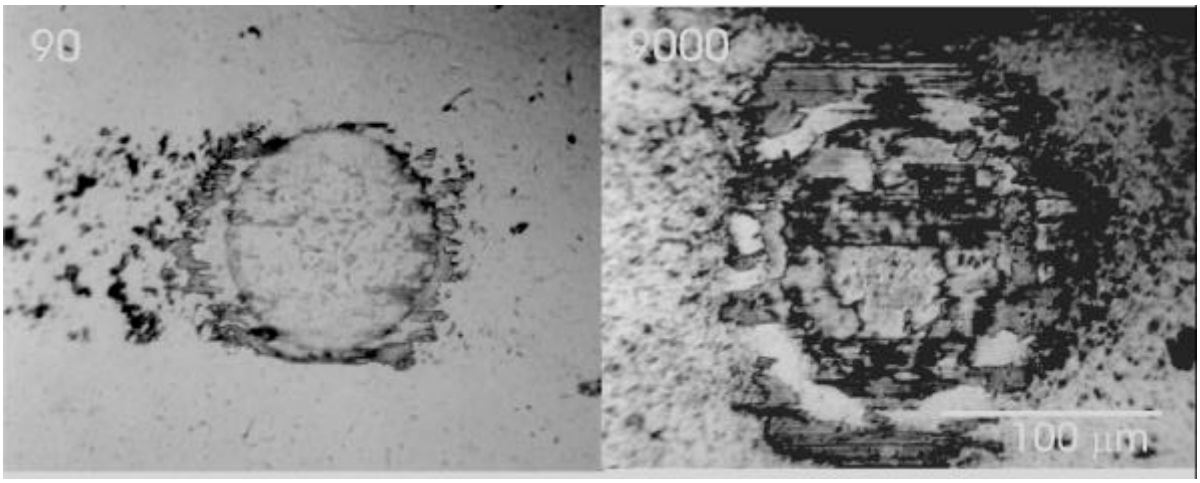

Figure 4. Optical micrographs of ball transfer films formed during sliding against IBAD MoS_2 coatings after (a) 90, and (b) 9000 sliding cycles.

The buildup and depletion of material on track and ball surfaces were quantified using EDS and are shown in Figure 5. As expected for dense coatings, material loss in the tracks is consistent with the optical interferometry results (Figure 2). On the balls, the average transfer film thickness in the center of the contact increased as sliding progressed. Thickness of ball transfer films at failure was not quantified due to oxygen incorporation, making it difficult to estimate thickness by EDS.

Most interesting was the buildup (Stage II) and then depletion (Stage III) of end patches found at the outermost turnaround points in the wear tracks (Figure 5, filled squares). From the plot, it can be seen that buildup occurred during the period of rapid coating loss from tracks in Stage II. Depletion

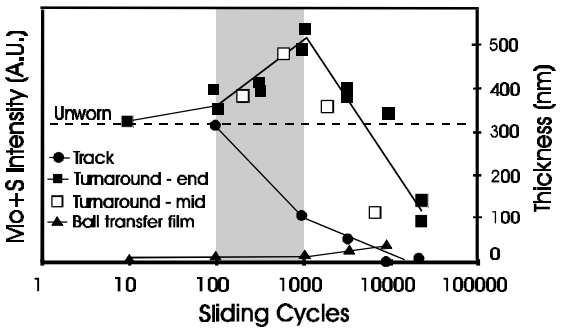

Figure 5. Track, patches at turnaround points (end and midpoints), and ball transfer film thickness measured by EDS.

of the end patches to nearly zero thickness occurred during the long steady state (low wear) Stage III. The patches at the center turnaround points, also shown in Figure 5 (open squares), were formed *after* the stroke length was shortened; consequently, these patches were accumulated on previously worn track surfaces. During the period of rapid coating wear (Stage II), these center patches were about the same thickness as those found at the outer endpoints. Conversely, the center patches in Stage III were thinner than the corresponding end patches. This is not unexpected, since the center patches were formed after the coating was substantially worn). However, these center patches are substantially thicker than the wear track on either side, therefore providing evidence that substantial lubricant redistribution *to as well as from* end patches continues after the high wear period.

4. DISCUSSION

The progression of third body wear morphology (Figures 3, 4), together with quantification of changes in thickness (Figure 5) are interpreted as a lubricant transfer process (Figure 6). During Stage I, a film transfers from the coating to the ball surface, and some of the lubricant is deposited in patches at the turnaround points, either directly (plowed) from the coating or indirectly (retransferred) from the ball transfer film (Figure 6a). In Stage II (Figure 6b), more of the lubricant

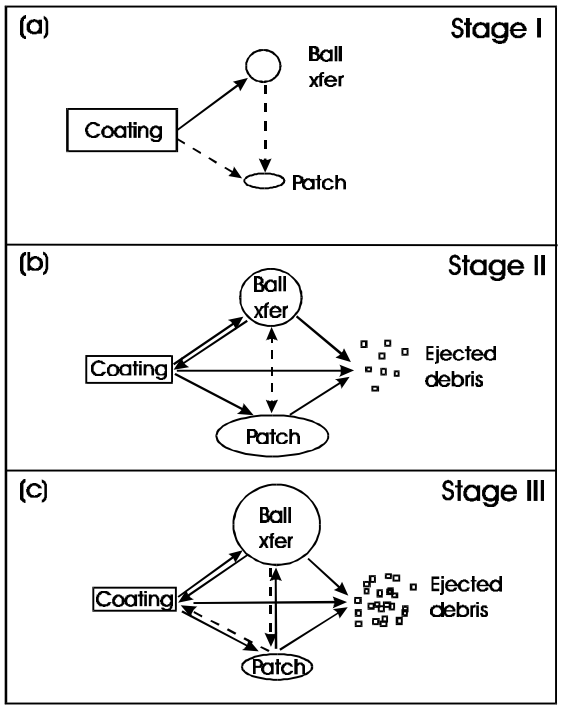

Figure 6. Schematic of lubricant transfer processes between the coating wear track (coating), ball transfer film (ball xfer), and patch material at turnaround points (patch) for (a) Stage I, (b) Stage II, and (c) Stage III sliding. Solid arrows indicate observed material transfer directions, while dashed lines indicate other possible transfer routes.

removed from the track is transferred to the patches at turnaround points as well as onto the ball. The material deposited at the turnaround points and on the ball surface can act as reservoirs to replenish lubricant lost from the sliding contact. During Stage III (Figure 6c), the end patches become depleted as they replenish lubricant to the sliding interface. Throughout Stages II and III, material is ejected (as loose debris) and lost to regions of the ball surface outside the contact zone as well as along the edges and beyond the ends of the tracks; this material is largely unrecoverable and is excluded from participation in the replenishment process.

We note that previous investigations of MoS_2 sliding have documented the individual processes described above. Transfer films are formed on the first pass [13,14,15], and MoS_2 debris can be extruded through the sliding contact and exchanged between transfer film and track surfaces [16,17]. Transfer film buildup has been correlated to lubricant loss in the track [4,13,14], and the importance of the transfer film for endurance of solid lubricants has long been noted by Lancaster [18].

Our experiments suggest the endurance is not simply determined by the wear rate of the MoS_2 coating, but rather by the dynamics of the replenishment process diagrammed in Figure 6. Together, the evolution of the thickness of transfer films, wear tracks, and end patches at turnaround points determine the net loss of material from the contact, not simply a coating wear rate. The amount of lubricant available to the contact is established by the dynamics of MoS_2 coating wear and replenishment. The model diagrammed in Figure 6 can be reduced semi-quantitatively to a simple summation of material fluxes J_{ij} (between coating, ball, end patches, and ejected debris), as shown in Figure 7.

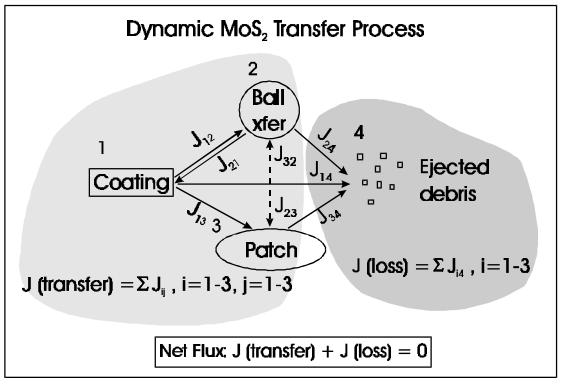

Figure 7. Semi-quantitative material transfer flux.

The models in Figures 6 and 7 are consistent with the third-body processes described by Godet [19,20]: 1) debris detaches from the first-bodies, 2) the debris is trapped in the contact, and 3) debris is ejected from the contact. In the simplest sense, it is this *loss flux* (or ejected debris) which is relevant to overall wear, rather than the individual particle detachment mechanisms observed. It is recognized that the material transfer process is influenced by particle entrapment in the contact, which in turn is influenced by such parameters as geometry, sliding configuration, and system vibration [20]. In our

configuration (ball-on-flat, bi-directional sliding) there are localized points on the track where lubricant material can build up. Unidirectional pin-on-disk and flat-on-flat test configurations would each have different entrapment geometries and rates. Interestingly, while the ability of MoS_2 debris to build up and remain entrapped in the contact may be beneficial in some cases, it is detrimental in others (e.g. torque-bumps formed on MoS_2 coated bearing surfaces during dithering [21]).

Finally, little is known about the third-body materials properties controlling these tribological interactions: mechanical properties, chemistry (bulk and interfacial), structure/phase, and morphology can contribute. If no chemical degradation is involved, the effective wear can be controlled by limiting the loss flux (J_{i4}~0), e.g., reducing either debris loss or debris generation rates. More detailed understanding of transfer film properties (mechanics, chemistry, etc.), coupled with an understanding of the lubricant transfer dynamics, can be used to guide modifications of solid lubricant chemistry or structure to enhance wear life and bearing performance.

5. CONCLUSIONS

A new methodology, 'stripe testing,' was used to study the wear behavior of thin, dense MoS_2 coatings. It was found that IBAD MoS_2 coatings wore rapidly during the first 5-10% of sliding life. Despite this early loss, lubrication of the sliding contact continued for the remaining 90% of sliding life. A dynamic transfer process was proposed, where third body lubricant reservoirs were formed, then emptied; this process provides replenishment by redistribution of lubricant between the track and ball surfaces. The dynamics of the process were inferred by coupling the stripe test methodology with quantitative measurement of material loss and buildup on the wear tracks and ball surfaces.

6. ACKNOWLEDGMENTS

The authors thank R.N. Bolster (Geo-Centers) for coating deposition, J.C. Wegand (Geo-Centers) for some tribotesting, and L.E. Seitzman (NRL) for valuable discussions.

REFERENCES

1. T. Spalvins, Thin Solid Films 118 (1984) 375.
2. G.D. Gamulya, G.V. Dobrovol'skaya, I.L. Lebedeva and T.P. Yukhno, Wear 93 (1984).
3. P.D. Fleischauer and R. Bauer, Tribol. Trans. 31 (1988) 239; M.R. Hilton, R. Bauer and P.D. Fleischauer, Thin Solid Films 188 (1990) 219.
4. I.L. Singer, S. Fayeulle and P.D. Ehni, Wear, in press.
5. G.B. Hopple, J.E. Keem, and S.H. Loewenthal, Wear 162-164 (1993) 919.
6. R.N. Bolster, I.L. Singer, J.C. Wegand, S. Fayeulle, and C.R. Gossett, Surf. Coat. Technol. 46 (1991) 207.
7. L.E. Seitzman, R.N. Bolster, I.L. Singer, and J.C. Wegand, Tribol. Trans. 38 (1995) 445.
8. L.E. Seitzman, I.L. Singer, R.N. Bolster and C.R. Gossett, Surf. Coat. Technol. 51 (1992) 232.
9. P.D. Ehni and I.L. Singer, Appl. Surf. Sci. 59 (1992) 45.
10. K.J. Wahl, L.E. Seitzman, R.N. Bolster, and I.L. Singer, Surf. Coat. Technol. 73 (1995) 152.
11. K.J. Wahl and I.L. Singer, Tribology Letters 1 (1995) 59.
12. S. Fayeulle, P.D. Ehni and I.L. Singer, in *Mechanics of Coatings*, Leeds-Lyon 16, Tribology Series 17, eds. D. Dowson, C.M. Taylor and M. Godet, Elsevier, Amsterdam, 1990, p. 129.
13. P.D. Fleischauer and R. Bauer, Tribol. Trans. 31 (1988) 239.
14. M.R. Hilton, R. Bauer, and P.D. Fleischauer, Thin Solid Films 188 (1990) 219.
15. P.D. Ehni and I.L. Singer, in *New Materials Approaches to Tribology: Theory and Applications*, Materials Research Society Symp. Proc., Vol. 140, eds. L.E. Pope, L. Fehrenbacher and W.O. Winer (Pittsburgh, 1989) p.245.
16. H.E. Sliney, ASLE Trans. 21 (1977) 109.
17. R.L. Fusaro, ASLE Trans. 25 (1982) 141; R.L. Fusaro, NASA TP-1343 (Cleveland, OH, 1978).
18. J. Lancaster, J. Tribol. 107 (1985) 437.
19. M. Godet, Wear 100 (1984) 437.
20. M. Godet, Wear 136 (1990) 29.
21. R. Bauer and P.D. Fleischauer, Tribol. Trans. 38 (1995) 1.

APPENDIX

A stepped-thickness coating of IBAD MoS_2 on Si was used for calibration of the Mo L_α + S K_α EDS signal. The thicknesses were measured optically by MI and were found to be 120, 235, 475, and 950 nm. The integrated peak area of the Mo+S signal vs. MoS_2 thickness at 20 keV is plotted in Figure A1. The data were fit using a linear least squares algorithm. Good correlation was found for thicknesses below 475 nm at 20 keV and 120 nm at 10 keV (not shown), with correlation coefficients 0.9995 and 0.995, respectively.

Since the substrates and balls used in the present experiment are steel, four further data points were acquired (at 20 keV) using various MoS_2 coatings between 55 and 440 nm thick deposited on 440C and 52100 steel substrates. These values are also plotted in Figure A1. As can be seen from the plot, the integrated intensities observed for MoS_2 on these steels are comparable to those observed for MoS_2 on Si.

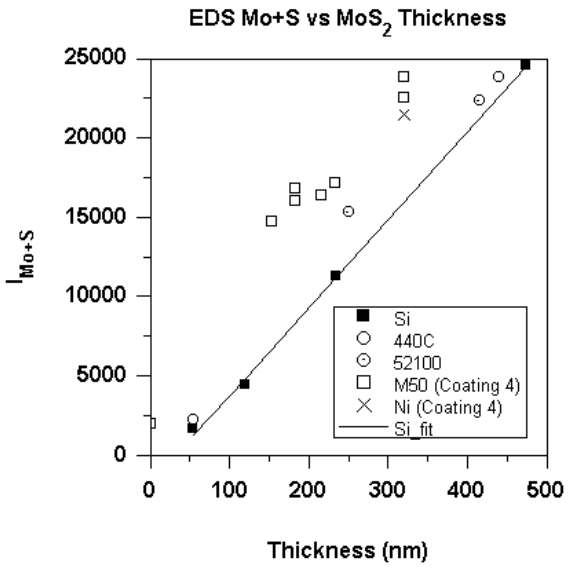

Figure A1. Quantification of EDS Mo+S signal as a function of MoS_2 coating thickness on Si substrate at 20 keV. Values for 4 coatings on steel substrates at 20 keV and the MoS_2 coating detailed in this study (on M50 and Ni substrates) are also shown.

The coating examined in this study was found by EDS to have a higher than average mass density given its measured thickness (see open squares in Figure A1). Additional data points for intermediate thicknesses were obtained using sputter craters measured by interferometry. Some enhancement of I_{Mo+S} can be attributed to the presence of about 2 at.% Mo in the substrate, which was M50 steel. However, this can only account for approximately 2000 counts for bare M50 and 800 additional counts at 320 nm. This was confirmed by the examination of the same coating deposited on a Ni foil, which results in only a small drop in intensity of the order expected (shown by X in Figure A1). The higher I_{Mo+S} signal of this coating as compared to the other coatings examined for the calibration was believed due to its being Mo-rich (e.g. MoS_{2-x}), which increases its effective density. This was consistent with the measured coating thickness vs. quartz crystal monitor mass data obtained during coating deposition.

Although the mass density of the coating examined in this study deviated from the norm, the thickness was still within the regime that can be approximated by a linear relationship. Since the coating is thin (320 nm), a large fraction of the 20 keV EDS signal comes from the substrate elements. Calibration for the dense film was obtained by subtracting the contribution to the I_{Mo+S} signal from the M50 steel; this was estimated by using the intensity ratio of Fe K_α to Mo L_α obtained from uncoated M50 steel and monitoring I_{Fe} across the worn surfaces. A corrected linear fit for the coating was then obtained, and these values used for quantification of wear track thicknesses.

EDS data from transfer films on the 52100 balls were obtained with 10 keV electrons because the films were too thin to be measured accurately using 20 keV electrons. At this lower beam energy, enhanced X-ray excitation cross-section allowed for better differentiation between small changes in thickness. Estimates of thicknesses were obtained by using the 10 keV calibration data from the MoS_2 coating on Si, but it is recognized that this probably overestimates the thickness by up to 20%. Thus, the thickness estimates of transfer films (which may be fluffy or porous) are used simply for comparative purposes. However, the changes in the mass thickness observed in a given region are real.